Proceedings of ASME Turbo Expo 2011
GT2011
June 6-10, 2011, Vancouver, British Columbia, Canada

GT2011-45073

PARAMETRIC STUDY OF FLUIDIC OSCILLATORS FOR USE IN ACTIVE BOUNDARY LAYER CONTROL

Marion Mack*
University of the German
Armed Forces Munich
Institute of Jet Propulsion
D-85577 Neubiberg
Germany
Email: marion.mack@unibw.de

Reinhard Niehuis
University of the German
Armed Forces Munich
Institute of Jet Propulsion
D-85577 Neubiberg
Germany
Email: reinhard.niehuis@unibw.de

Andreas Fiala
MTU Aero Engines GmbH
Dachauer Str. 665
D-80995 Munich
Germany
Email: Andreas.Fiala@mtu.de

ABSTRACT

A parametric study was conducted to identify the main factors influencing the frequency produced by fluidic oscillators with the goal of using the actuator to trigger boundary layer transition through the excitation of Tollmien Schlichting waves. Test bench conditions were chosen to match the static pressure at the actuation position on the candidate blade profile for a cascade exit Mach number of 0.6 and Reynolds numbers from 60,000 to 200,000. The inlet vs. outlet pressure ratio and the position and geometry of the outlet holes were all varied. Additionally, the effect of the oscillator's scale and the feedback channel geometry were considered. The flow at the exit was measured using a hot wire, while Kulite pressure transducers were used to measure pressure fluctuations within the device. This paper shows that fluidic oscillators can achieve frequencies of 10 kHz and that the parameters considered play an important role in the performance of these devices.

NOMENCLATURE

$c_p = \frac{p-p_k}{p_{t1}-pk}$ pressure coefficient
d diameter of outlet holes
f frequency
$H_k = \delta^*/\theta$ shape factor for incompressible flow
l outlet length
L length from nozzle to splitter
l_f feedback channel length
$\dot{m}$ mass flow
Ma Mach number
p_k static pressure inside the pressure tank
p_t total pressure
R pressure ratio p_{t0}/p_k
Re Reynolds number
U velocity
δ^* displacement thickness
ν kinematic viscosity
$\omega = \frac{2\pi\nu_e}{u_e^2}$ non-dimensional disturbance frequency
θ momentum thickness
τ oscillation period
τ_s switching time
τ_t transmission time
$\zeta = \frac{p_{t2}-p_{t1}}{p_{t1}-p_k}$ loss coefficient

Subscripts

$aimax$ maximum temporal amplification factor
$chord$ referring to chord length
e state at the edge of the boundary layer
e state in the pressure tank
0 state in the pressure reservoir
1 state at the actuator resp. cascade inlet
2 state at the cascade exit
ref conditions at aerodynamic design point

*Address all correspondence to this author.

INTRODUCTION

In order to reduce weight and maintenance costs of the low pressure turbine, current design philosophies aim at reducing the blade numbers by using high lift blade profiles with an increased pitch-to-chord ratio. This design principle leads to strong adverse pressure gradients and thus to the danger of boundary layer separation on the suction side of the profile which in turn leads to increased aerodynamic loss. It has been shown recently that these losses can be reduced through the application of passive and active boundary layer control.

Several forms of passive turbulators have been found to be effective, especially for steady inflow conditions at low Reynolds numbers below 100,000 by Sieverding et al. [1] and Rouser et al. [2]. Under periodically unsteady inflow conditions typical of real turbomachinery and at higher Reynolds numbers passive boundary layer control has negative effects as it can cause an increase in the profile losses, see e.g. Martinstetter et al. [3] [4], Zhang and Hodson [5], and Himmel et al. [6].

Passive boundary layer control cannot be deactivated under circumstances where it is not needed. Since modern low pressure turbines typically operate under a wide range of Reynolds numbers, this is a major disadvantage. Active boundary layer control systems, being able to be deactivated at non-critical conditions, show a higher flexibility, as shown by Schumann et al. [7] and Garg [8].

Steady blowing from a row of holes would be a relatively simple system to implement, as the technology is well known from blade cooling assemblies. Investigations on control effectiveness and blowing position have been performed by Zheng et al. [9] and McAulliffe and Sjolander [10]. Ludewig et al. [11] documented the importance of inflow conditions and blowing ratio on the effect of steady blowing. Although separation can be successfully suppressed, the required mass flow for good control performance is comparatively high for steady blowing. Opportunities for improvement are especially prevalent at low Reynolds number operation.

Low frequency $(\leq 100Hz)$ pulsed blowing, as applied by Bons et al. [12] and Lengani et al. [13] significantly reduced the required injection mass flow while still maintaining good control performance. Another promising approach is the excitation of Tollmien-Schlichting waves to trigger transition to turbulence, thus increasing the boundary layer's ability to stay attached, as proposed by Ries et al. [14]. This calls for a dramatically different pulsing technique, as for realistic turbomachinery conditions, the frequencies are several orders of magnitude higher than those tested by Bons et al. [12] and Lengani et al. [13]. This paper aims at determining parameters for a fluidic oscillator similar to the one proposed by Ries et al. [14] that will provide effective separation control for a high-lift, state of the art, low pressure turbine profile (Gier et al. [15]).

TABLE 1. f_{aimax} AT THREE SELECTED LOCATIONS ALONG THE SUCTION SIDE OF A TYPICAL HIGH-LIFT LPT BLADE AT $Re_{chord} = 200000$

H_k	$Re_{\delta *}$	$U_e[m/s]$	$\omega_{aimax} * 10^4$	$f_{aimax}[kHz]$
2.591	750	242.1	1.38	15.4
2.801	844	240.6	1.07	11.8
4.029	1383	235.7	0.82	8.8

TABLE 2. f_{aimax} AT THREE SELECTED LOCATIONS ALONG THE SUCTION SIDE OF A TYPICAL HIGH-LIFT LPT BLADE AT $Re_{chord} = 50000$

H_k	$Re_{\delta *}$	$U_e[m/s]$	$\omega_{aimax} * 10^4$	$f_{aimax}[kHz]$
2.591	370	241.0	-	-
2.801	420	239.5	3.32	36.5
4.029	695	235.9	2.34	25.0

ASSESSMENT OF OPTIMAL FREQUENCIES FOR HIGH LIFT LPT BLADE

Before tests on the blade can be carried out, optimal frequencies need to be assessed for different Reynolds numbers. Starting with the displacement thickness δ^* distribution along the suction side the displacement Reynolds-number Re_{δ^*} is selected at locations close to maximal velocity, at laminar separation, and at a location in between. Together with the incompressible form factor H_k at these locations, three characteristic frequencies can be identified for each velocity profile from the Spatial Stability Charts of Tollmien Schlichting waves after Wazzan et al. [16]. These are the highest and lowest frequency at which a disturbance cannot be amplified and the frequency where maximal amplification occurs. The latter frequency is given in table 1 for the three selected locations at $Re_{chord} = 200,000$. The boundary layer values have been derived from DLR's Navier-Stokes solver TRACE [17] and for comparison with one of MTU's boundary layer codes UBLIM [18]. For $Re_{chord} = 50,000$ in table 2 the frequency reveals an increased value because the higher boundary layer thickness at the lower Reynolds number does not compensate the decrease in Reynolds number. At the location of maximum velocity no amplification is possible for $Re_{chord} = 50,000$. From this comparison it is evident that very high frequencies are necessary for an optimal effect of pulsed blowing at high Mach numbers and low Reynolds numbers.

FLUIDIC OSCILLATORS

The working principle of a fluidic oscillator can be explained with the aid of figure 1. A jet entering the oscillator through the nozzle attaches to one of the diverging walls due to the Coanda effect and enters primarily into one of the feedback channels separated by a splitter, causing a higher stagnation pressure inside that feedback channel. As the higher pressure reaches the nozzle through the feedback channel, it causes the jet to attach to the other wall. In the second feedback channel this loop is repeated causing the jet to oscillate between both walls. For the oscillators considered in this paper, the flow leaves the oscillator through one hole in each feedback channel at an angle to the oscillator plane, as shown in fig. 2, thus being subjected to the pressure fluctuations in the feedback channel which lead to an oscillating mass flow through the outlets. Oscillators with the flow leaving in a straight line from the nozzle in the oscillator plane have been examined in detail in open literature.

Wright [19] describes the frequency of a single configuration as linearly dependent on the mass flow, Yang et al. [20], Khelfaoui et al. [21] and Chen et al. [22] as linearly dependent on volume flow. Ries et al. [14] performed numerical investigations on frequency and oscillator size, which show that very high frequencies can be achieved. According to Simões et al. [23] and Gebhard et al. [24], the oscillation period τ can be divided into the switching time τ_s that it takes the jet to switch from one attachment wall to the other, and the transmission time τ_t needed for the pressure to propagate through the feedback channel to the nozzle. Both state that the propagation of the pressure rise through the feedback channel occurs with speed of sound, while switching time depends on jet velocity, nozzle and splitter design, and nozzle to splitter distance. Thus, switching time is the dominant factor for oscillation frequency.

To the authors' knowledge, in all available literature except Ries et al. [14] fluidic oscillators are described with the flow exiting in a straight line from the nozzle in the oscillator plane. In order to reduce installation space, a fluidic oscillator is proposed with the flow leaving the feedback channel in a direction perpendicular to the oscillator plane. Preliminary studies with this kind of oscillator conducted by the authors showed an influence of the outlet geometry and discrepancies with the results of Ries et al. [14], making it impossible to use their results in the current design. In order to select a suitable oscillator for cascade tests, a thorough parametric study was conducted.

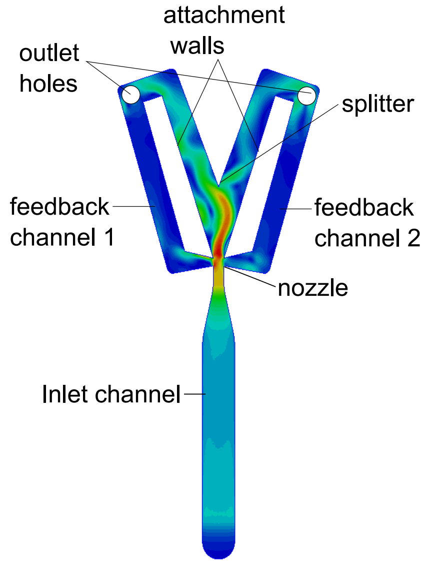

FIGURE 1. WORKING PRINCIPLE OF A FLUIDIC OSCILLATOR

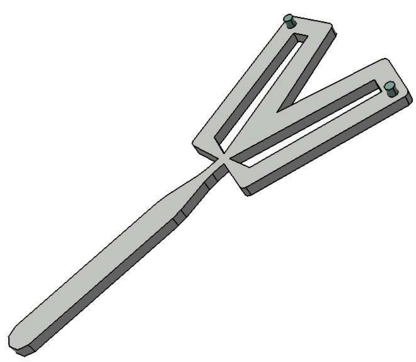

FIGURE 2. INNER STRUCTURE OF A FLUIDIC OSCILLATOR

EXPERIMENTAL SETUP

The High-Speed Cascade Wind Tunnel

The experiments were conducted at the High-speed Cascade Wind Tunnel of the Institute of Jet Propulsion which is shown in figure 3. The wind tunnel is a continuously operating open-loop wind tunnel which, except for the driving unit, is located inside a pressure tank. The drive unit consists of a 1.3 MW electric motor, a hydraulic coupling and a gearbox. Two vacuum pumps are used to evacuate the tank to a static pressure between 4000 Pa and atmospheric pressure. By varying the pressure inside the tank, Reynolds and Mach number can be varied independently. The driving unit drives a six-stage axial compressor. The flow from the compressor passes through a cooler and a settling chamber before being accelerated in the nozzle towards the test section, where the cascade is placed.

For the parametric study, the wind tunnel was used solely as a pressure chamber. The actuators were mounted inside the pressure tank, which was evacuated to pressures between 50 and 300 mbar which are the expected static pressure levels at the ejection location on the blade during the tests. Ambient air was fed to the actuator via a valve that served as throttle to adjust the pressure in

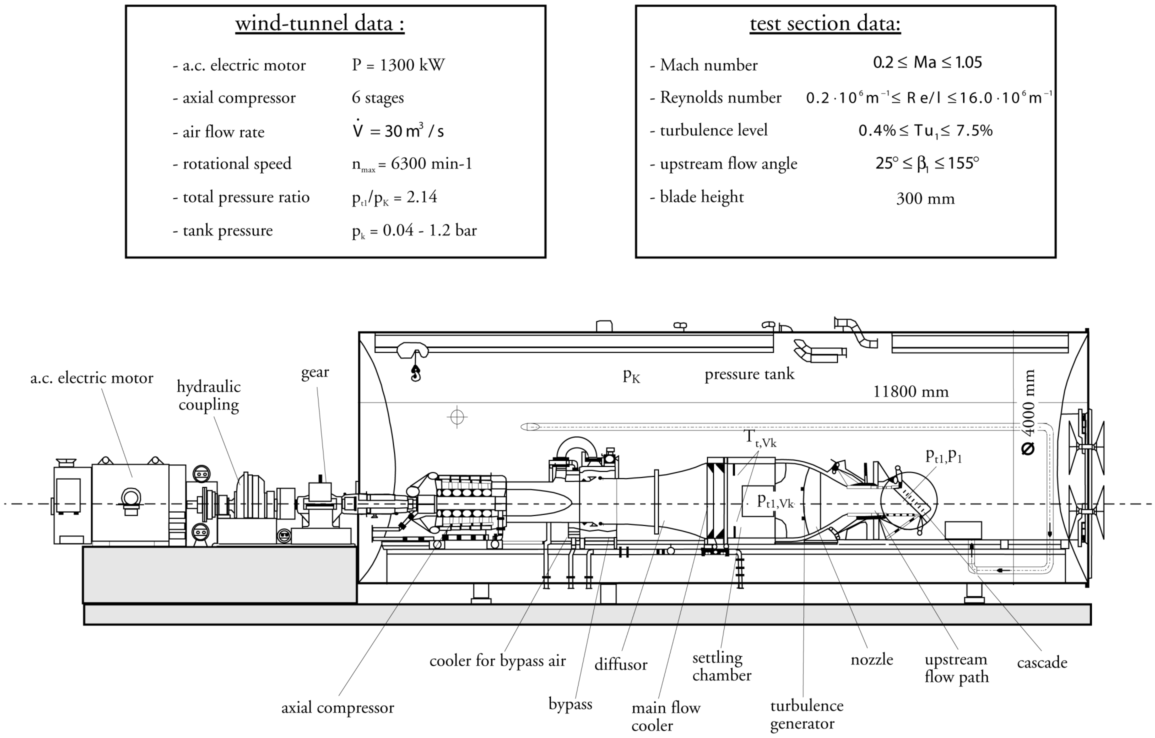

FIGURE 3. THE HIGH-SPEED CASCADE WIND TUNNEL

the pressure reservoir to the desired level. As the pressure reservoir was orders of magnitude larger than the actuator volume, the pressure measured was considered to be the total pressure. At the actuator inlet, the static pressure was measured and at the outlets, the flow velocity was measured with a hot wire probe, as shown in figure 4.

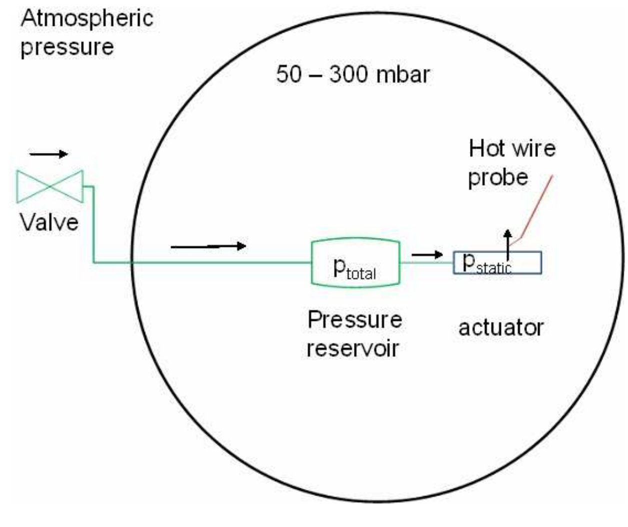

FIGURE 4. TEST SETUP FOR PARAMETRIC STUDY

Fluidic Oscillators

Two different basic layouts of fluidic oscillators were tested according to table 3. The first layout was similar to the one numerically investigated by Ries et al. [14] and was tested in two sizes (type A and B) and the second layout (type C) had shortened feedback channels and nozzle-splitter distance. All three configurations can be seen in figure 5. The tank pressure, the pressure ratio R and the geometry of the outlets were varied for each of these types. For type A, a shortened inlet channel was tested to assess the possibility of further reducing installation space.

Tank pressure levels were 50 mbar, 100 mbar, 150 mbar, 200 mbar and 300 mbar.

The pressure ratio R was studied in a range from 1.4 to 4.4.

Four outlet positions which 2 outlet holes open for each configuration were tested for type A. Based on these results, three hole positions for type B and two hole positions for Type C were tested, as shown in figure 6.

The outlets' length/diameter ratio was varied from 3 to 13.

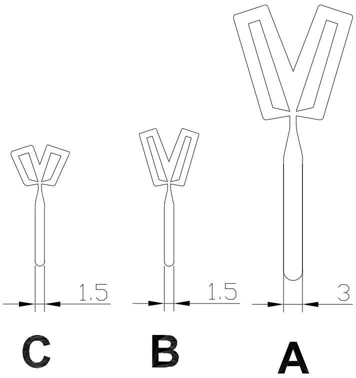

FIGURE 5. EXAMINED BASIC GEOMETRIES

TABLE 3. OVERVIEW OF THE EXAMINED CONFIGURATIONS

Layout	Outlet Positions	l/d ratios
A	1, 2, 3, 4	3.75, 4.29, 5, 6.25, 7.14, 8.33
B	1, 2, 3	3, 5, 6.25, 8.33, 10, 12.5, 16.67
C	1, 3	5, 10

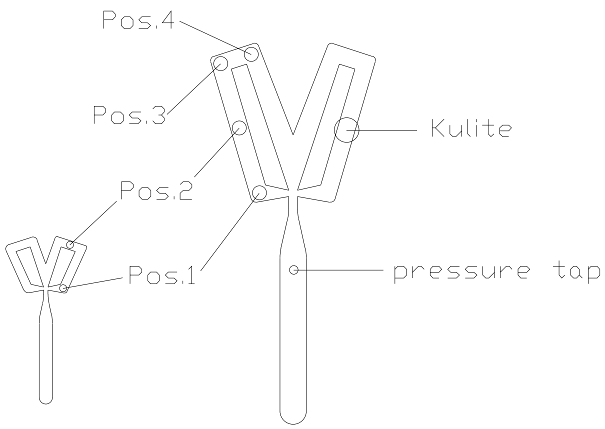

FIGURE 6. OSCILLATORS WITH INSTRUMENTATION AND POSSIBLE OUTLET POSITIONS

Assembled Cascade

After the parametric study itself, a setup was chosen to be incorporated into a low pressure turbine blade. The blade was equipped with a row of oscillators as shown in figure 7 and installed in a cascade which was then mounted into the High-speed Cascade Wind Tunnel. The oscillators were connected to a plenum inside the blade that was supplied with ambient air by a throttle valve.

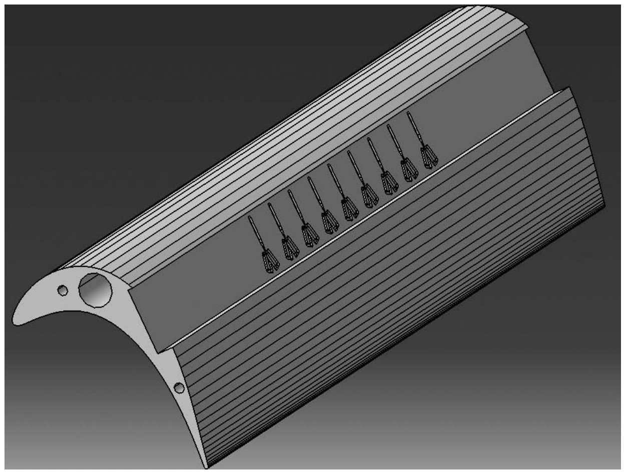

FIGURE 7. CUTAWAY OF BLADE, SHOWING THE ROW OF OSCILLATORS

Instrumentation

As shown in figure 6, the base plates of types A and B were instrumented with a pressure tap of 0.6 mm diameter in the inlet channel as well as with a Kulite pressure transducer XCW-093 allowing time resolved measurements up to frequencies of 150 kHz. For type C, only frequency at the outlet was measured with CTA. Kulite and CTA measurements were conducted within a few seconds of each other.

In order to gain information about the effectiveness of the fluidic oscillators, measurements of a cascade consisting of seven LPT blades of which the centre 3 blades were equipped with fluidic oscillators were conducted. The blades adjacent to the centre blade were equipped with static pressure taps in the midspan region. Pressure taps were located at 20 axial positions on the suction side and at 6 axial positions on the pressure side, where no effect was expected. The wake of the central blade is analyzed by traversing a five-hole-probe over one cascade pitch 40% axial chord length downstream the centre blade exit plane. The plenum pressures were measured in order to determine the pressure ratio driving the actuator.

All pressures were measured by means of a *Pressure Systems RK98* pressure scanner controlled by in-house software. Data from the Kulite sensor was acquired at a sampling rate of 100 kHz using a custom amplifier and a National Instruments A/D converter board and stored with in-house software. In addition to the pressure signals, the exit frequency was measured using constant temperature hot-wire anemometry (CTA). A miniature single-wire probe type *55P11* from Dantec was placed over the

centre of the outlet. For the measurements on the assembled blades, only CTA was used. Again, a miniature single wire probe was centred over an outlet. The data acquisition included a 30 kHz lowpass filter in order to avoid aliasing effects. Data was taken at a sampling rate of 60 kHz for a period of two seconds.
The effective length of the hot-wire of 1.25 mm is bigger than the diameter of the outlet, which never exceeded 1 mm. Thus, the probe could not be calibrated, as only a part of the wire was exposed to the flow. Accordingly, no information on oscillation amplitude could be gained. Further processing of the Kulite and CTA signals consisted of an FFT to extract the frequency information from the time signal. As the mass flow was too small to measure it with available equipment, the pressure ratio R=p_{t0}/p_k was chosen as indicator for the mass flow.

RESULTS

The initial results presented here focus on a single oscillator under quiescent conditions. The last two parts of this section will show how a cross flow affects oscillator performance and a preliminary analysis of loss measurements performed on a cascade with and without fluidic oscillators activated.

Frequency of the Oscillator Measured at Different Locations by Different Techniques

The acquired frequencies from CTA and Kulite show slightly different characteristics. Examples of both signals can be seen in figures 8 and 9. Both Kulite and CTA signal show one fundamental frequency and several harmonics. As can be seen by comparing figures 8 and 9, the dominating frequencies measured with both techniques coincide well. This is the case for all measurements (data not shown), so both measurement techniques can be used to assess the oscillating frequency. Unless otherwise explicitly stated, frequencies given refer to the fundamental frequency and were taken from CTA measurements.

Variation of Geometry

Figure 10 shows the frequency's dependence on oscillator size. As expected, the highest frequencies can be obtained with type C, which is equipped with the shortest feedback channels and nozzle to splitter distance L. L decreases by a factor of 0.84, the feedback channel length decreases by a factor of 0.75. If, as predicted by Gebhard et al. [24], the frequency is mainly dependent on the nozzle to splitter distance, the frequency should increase by a factor of 1/0.84=1.19. The ratio between the maximum frequencies for type B and C is 1.18, with both frequencies being achieved with very similar outlet configurations. Taking into consideration the fact that the splitter angle has changed and that both frequencies were recorded at slightly different pressure

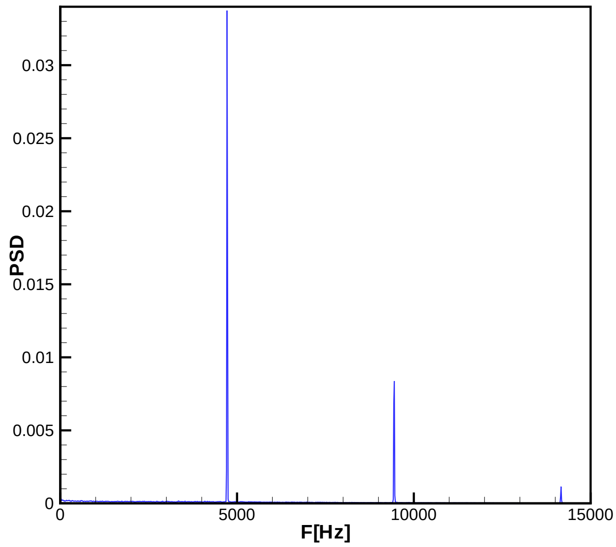

FIGURE 8. CTA SIGNAL FOR TYPE A ACTUATOR WITH l/d=10 AT A TANK PRESSURE OF 150 mbar

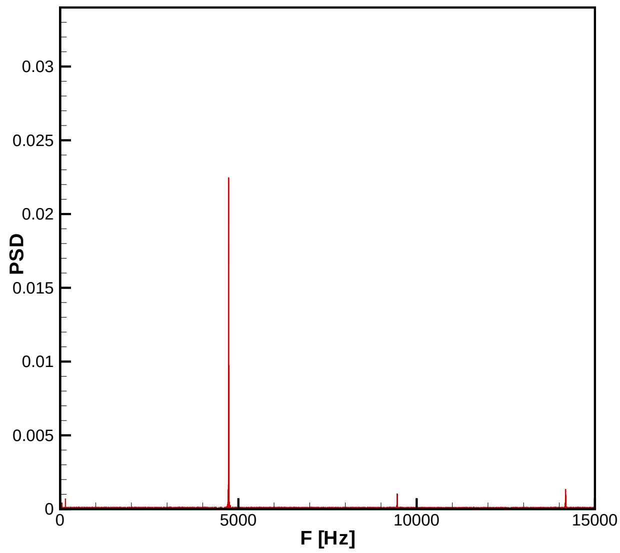

FIGURE 9. KULITE SIGNAL OF THE SAME CONFIGURATION AS IN FIG. 8

ratios but otherwise identical configurations, this seems to confirm that for a given oscillator configuration with respect to outlet geometry the relation of Gebhard et al. [24] is valid. However, the same comparison between type A and B shows strong deviations from this relation which raises doubt about the validity of the relation.
Experiments with a shortened inlet channel confirmed that the inlet length could be reduced by a factor of three with no effects

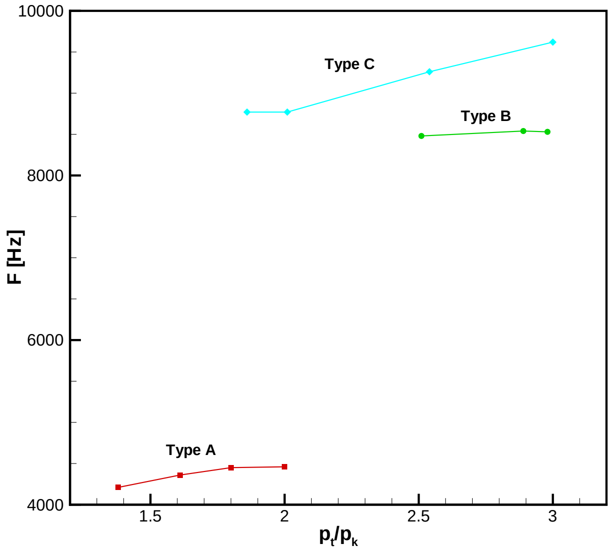

FIGURE 10. EFFECT OF BASIC GEOMETRY ON FREQUENCY

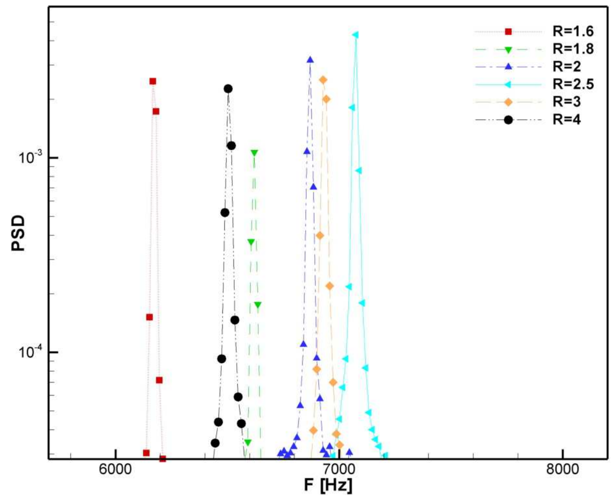

FIGURE 11. EFFECT OF PRESSURE RATIO ON FREQUENCY

on oscillation onset or frequency (results not shown).

Influence of Pressure Ratio R

One of the main influence factors on oscillation frequency is known to be the volume flow, which is strongly coupled to the pressure ratio R. Due to the high total pressure losses in the supply pipe from the pressure reservoir to the fluidic oscillator as well as in the fluidic oscillator itself, R can by far exceed the critical pressure ratio for air without choke condition occurring anywhere within the fluidic oscillator, which makes values for R of 2 and more possible.

Figure 11 shows the effect of R on the oscillation frequency. As expected, once oscillation is established, the frequency increases with R in a non-linear way, as the relationship between R and $\dot{m}$ is non-linear. Surprisingly, the frequency reaches a maximum and starts to decrease with increasing mass flow. By approximating the total pressure loss in the supply line, the flow velocities at the pressure tap's location can be estimated to be in a range where choking at the nozzle is a possibility. As figure 12 shows, there is also a relation between outlet diameter and the pressure ratio where maximum frequency is reached. Although the mechanism for the decreasing frequency is unknown, this might be due to choking at the outlet. Although the cross-section of both outlets combined is bigger than that of the nozzle, the cross section of one outlet hole is smaller than that of the nozzle for some configurations. If a significant fraction of the mass flow participates in the oscillation, this could cause choking at the outlet while the nozzle does not experience choking condition. Further study is needed to understand this phenomenon.

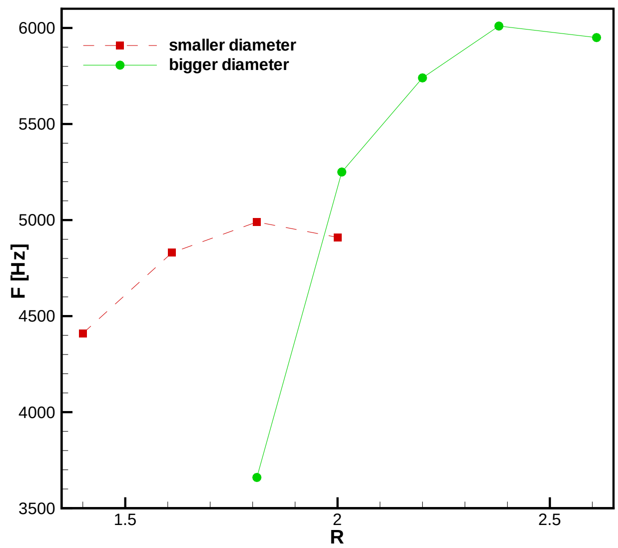

FIGURE 12. LOCATIONS OF MAXIMUM FOR TWO DIFFERENT DIAMETERS

Outlet Position and Length to Diameter Ratio

As preliminary studies performed by the authors showed, the geometry of the outlets is an important factor for the oscillation frequency. A main deciding factor turned out to be the length to diameter ratio l/d of the holes. Figure 13 shows the frequencies that were achieved for actuator configurations with different length to diameter ratios averaged for all pressure ratios and tank pressure levels. As can be seen, for type C as well as type B, there is a maximum at l/d=5. For Type A, the highest oscillation frequencies are reached for l/d=8.33.

The position of the outlets was varied as shown in figure 6in order to assess its effects on the oscillation. Figure 14 shows the results of measurements on the type A actuator. As can be seen, the maximum frequency that can be obtained varies only slightly. For positions one to three, the differences are small. At position four, however, the oscillation took place at a very low frequency for most configurations and pressure ratios, only occasionally reaching higher frequencies. As position four is at the first bend after the splitter, see figure 6, the most plausible explanation is that on this position, the interaction between jet and outlet is substantially different from the interaction between the jet and the outlet when they are not in line of sight.

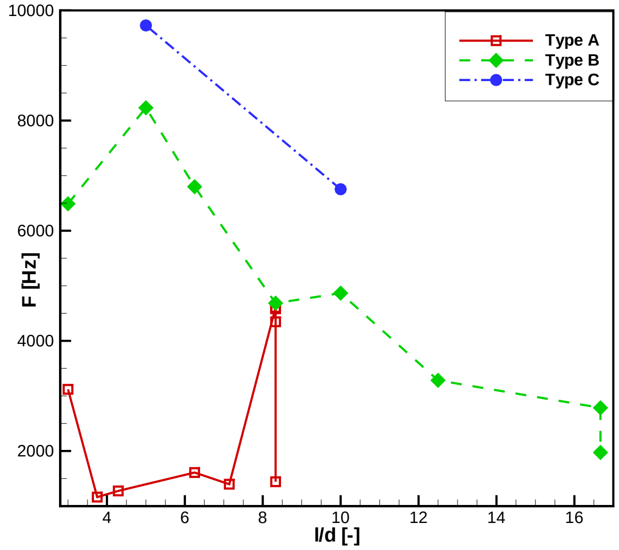

FIGURE 13. ACHIEVED AVERAGE FREQUENCIES AT DIFFERENT LENGTH TO DIAMETER RATIOS

Ambient Pressure

Dependence on the ambient pressure was a concern, as the actuators have to work at exit pressures as low as 50 mbar. Therefore, the ambient pressure inside the wind tunnel chamber was varied between 50 mbar and 300 mbar. Figure 15 shows the effect of the tank pressure for one configuration of the type A actuator. Frequency varies by no more than 100 Hz. For different configurations, the results were basically the same, showing no significant and clear trend that could be caused by the tank pressure. Overall, the obtained frequencies especially of the type C actuator are in a range that seems acceptable for the planned cascade tests.

Although the effect of tank pressure on oscillation frequency is weak, there is a strong effect on the onset of oscillation. The necessary pressure ratio for starting an oscillation increased with decreasing tank pressure. At 50 mbar, the oscillation was hard to start, unstable and, under some configurations of type B and C, did not occur at all. In the cases where fluctuation did not start, Re_1 was lower than 570. For all cases that started fluctuation, Re_1 was higher than 630, with Re_1 calculated by using a total pressure loss that was approximated based on the supply tube length and diameter, neglecting the exit from the pressure reservoir and the entry into the actuator itself. This behaviour is analogous to that described by Schreck and Schäfer in [25] for a sudden expansion of a channel, where asymmetrical behaviour starts at a Reynolds number depending on the geometry of the expansion.

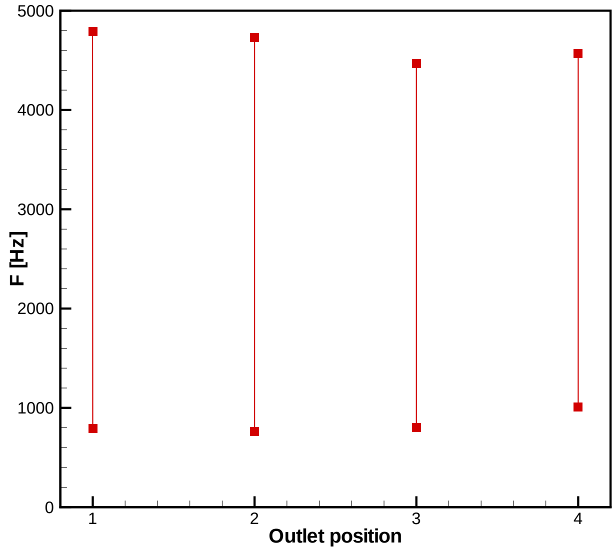

FIGURE 14. ACHIEVED FREQUENCY RANGES FOR A FLUIDIC OSCILLATOR TYPE A AT ALL 4 OUTLET POSITIONS

RANDOM FLUCTUATION OF OSCILLATION FREQUENCY

In addition to relatively stable oscillations in the actuator, it was also observed that for one configuration of type B with very high l/d at high pressure ratios, the oscillation switched randomly between two discrete frequencies. For low pressure ratios, the lower frequency dominated, with increasing pressure ratio the percentage of the higher frequency rose until it completely dominated. Figure 16 shows the transition between the two frequencies. The frequencies appear to be coupled by a factor of very near 4, being 2120Hz and 8610Hz. Apparently, the actuator switches between two modes of oscillation . Although obviously related to the outlet diameter and the pressure, it is not known what causes this behaviour or if and how it could be triggered to be taken advantage of.

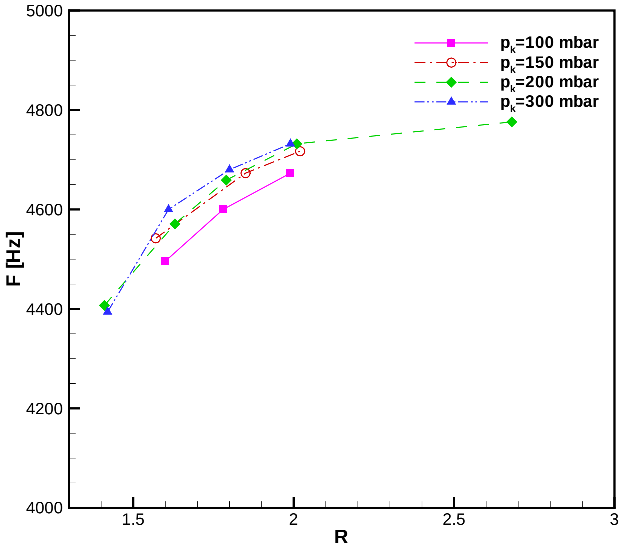

FIGURE 15. OSCILLATION FREQUENCY IN DEPENDENCE OF R FOR DIFFERENT PRESSURES AT OUTLET OF AN ACTUATOR TYPE A

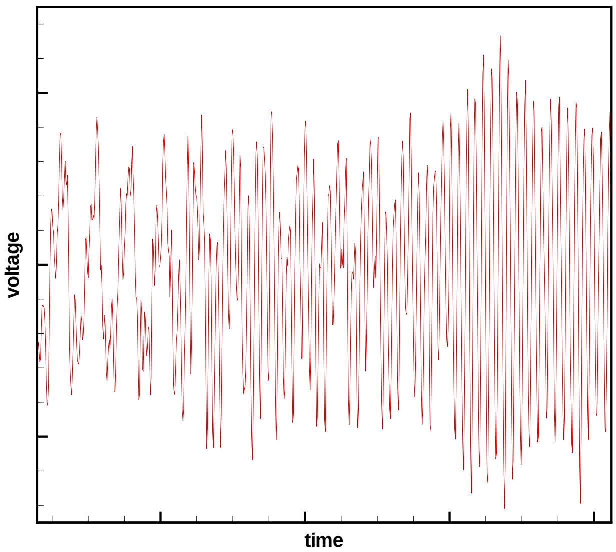

FIGURE 16. KULITE SIGNAL OF THE TRANSITION BETWEEN TWO FREQUENCIES AT HIGH R

Influence of Cross Flow

After the parametric study, a type C actuator with l/d= 5, outlet at position 2 and a short inlet channel was selected for incorporation into a LPT cascade. The cascade was tested at several operating points to evaluate the influence of the cross flow on the oscillation. In contrast to the case without cross flow, oscillation could be initiated for pressures at the outlets as low as 45 mbar, and, as can be seen in figure 17, showed no indication of noteworthy harmonics. The cross flow seems to have a stabilizing effect on the oscillation and to suppress the harmonics. A possible explanation for the latter is that the flow dampens frequencies that it is not receptive to.

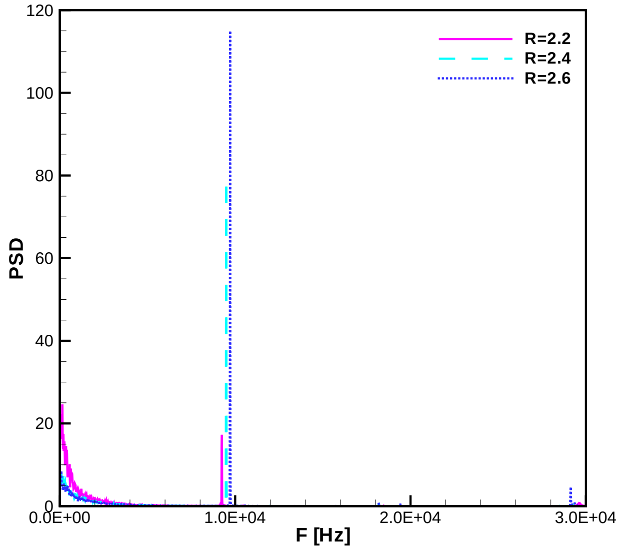

FIGURE 17. OSCILLATION AT 50 mbar EXIT PRESSURE WITH CROSS FLOW AT Ma=0.7

Cascade Measurements

To show effectiveness of active boundary layer control with fluidic oscillators, the profile pressure distribution and the midspan wake were measured for $Re = 90000$ and $Ma = 0.6$ where separation is known to occur at the examined LPT blade. Measurements were taken with the actuators deactivated and driven by two distinct pressure ratios. As shown in figure 18, without actuation a separation region occurs and this can be significantly reduced in size by activating the fluidic oscillators. The improvement is the same in both controlled cases. The results of the wake measurements are shown in figure 19, where the local loss coefficient for a wake traverse is standardized to the maximum local loss coefficient at the aerodynamic design point without actuation. While both pressure ratios reduce the size of the wake, the biggest decrease is achieved by blowing with the lower pressure ratio. This indicates that there is an optimum pressure ratio for loss reduction.This optimum as well as the performance of the oscillating actuators in the presence of unsteady inflow conditions will be the topics of discussion in upcoming papers.

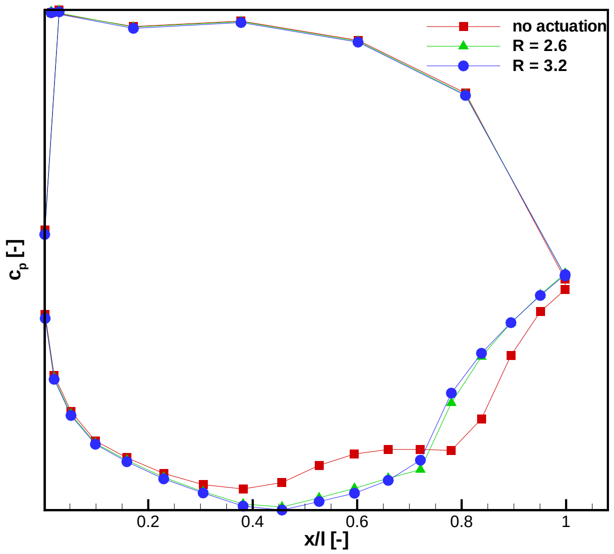

FIGURE 18. PROFILE PRESSURE DISTRIBUTION OF THE LPT BLADE WITH AND WITHOUT ACTUATION

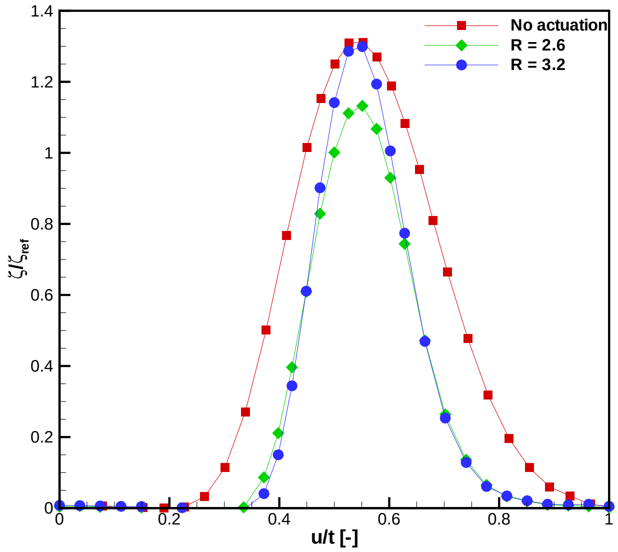

FIGURE 19. MIDSPAN WAKES OF THE LPT BLADE WITH AND WITHOUT ACTUATION

CONCLUSION

Fluidic oscillators with the flow exiting the feedback channels perpendicular to the oscillator plane have been examined with respect to a possible application as a source of pulsating active flow control for a low pressure turbine blade. The range of frequencies needed for optimum actuation performance was assessed and the frequencies achievable for different configurations were determined. A detailed parametric study was conducted in order to assess the importance of several factors. A test with oscillators incorporated into a LPT blade was conducted to determine effects of cross flow.

CTA and kulite sensors were found to coincide well in terms of the fundamental oscillation frequency. Fluidic oscillators on a scale as considered in this paper are capable of producing oscillation frequencies up to 10 kHz. It is a reasonable assumption that further downscaling and geometry optimization can increase the frequencies yet further. Candidates for optimization are the nozzle-splitter distance, the splitter angle and the geometry of the outlets. The outlet position needs to be behind the first bend after the splitter for reliably high frequencies, while exit pressure has influence on the onset and stability of the oscillation. Cross flow over the actuator effectively suppresses higher harmonics that occur when blowing into still air.

Fluidic oscillators show a reduction of the separation region and of profile losses under steady inflow conditions and seem to have an optimum pressure ratio above which losses increase again. Further investigations will focus on determining the optimum pressure ratio and extend experiments to unsteady inflow conditions.

In order to fully understand the performance of fluidic oscillators with perpendicular outlets, further work, both experimental and numerical, is necessary. Experiments on a larger scale can serve to study more parameters, e.g. the depth of the oscillator, and to determine influence factors for the oscillating percentage of the flow. An accurate numerical model or flow visualization can help to understand the interaction of the oscillator with the outlets or phenomena like the frequency maximum, the harmonics vanishing in cross flow and the switching between two discrete frequencies.

ACKNOWLEDGMENT

The research leading to these results has received funding from the European Union Seventh Framework Programme (FP7/2007-2013) under grant agreement n 211861, DREAM. We would like to thank our fellow partners in the European Union FP7 Programme DREAM for permitting the publication of our results in this paper.

REFERENCES

[1] Sieverding, C. H., Bagnera, C., Boege, A. C., Anton, J. A. C., and Luere, V., 2004. "Investigation of the Effectiveness of Various Types of Boundary Layer Transition Elements of Low Reynolds Number Turbine Bladings". In ASME Paper GT2004-54103.

[2] Rouser, K., King, P., and Sondergaard, R., 2003. "Effect of Dimples on Boundary Layer Separation on a Low Pressure Turbine Blade". In ISABE Paper, ISABE-2003-1097.

[3] Martinstetter, M., Niehuis, R., and Franke, M., 2010. "Passive Boundary Layer Control on a Highly Loaded Low Pressure Turbine Cascade". In ASME Paper GT2010-22739.

[4] Martinstetter, M., 2010. "Experimentelle Untersuchungen zur Aerodynamik hoch belasteter Niederdruckturbinen-Beschaufelungen". PhD thesis, University of the German Armed Forces Munich.

[5] Zhang, X. F., and Hodson, H., 2005. "Combined Effects of Surface Trips and Unsteady Wakes on the Boundary Layer Development of an Ultra-High-Lift LP Turbine Blade". *Journal of Turbomachinery,* ***127***(3), pp. 479–488.

[6] Himmel, C., Thomas, R., and Hodson, H., 2009. "Effective Passive Flow Control For Ultra-High Lift Low pressure Turbines". In ETC 2009 Paper No.130.

[7] Schumann, T., Rose, M. G., Staudacher, S., Gier, J., and Schröder, T., 2008. "The Effects of Steady Injection on an Ultra High Lift Vane in a LP Turbine". In ASME Paper GT2008-50330.

[8] Garg, V., 2002. "Low-Pressure Turbine Separation Control: Comparison With Experimental Data". In ASME-Paper GT2002-30229.

[9] Zheng, X., Zhang, Y., Xing, W., and Zhang, J., 2007. "Separation Control of Axial Compressor Cascade by Fluidic-Based Excitations". In ASME-Paper GT2007-27560.

[10] McAuliffe, B. R., and Sjolander, S. A., 2004. "Active Flow Control Using Steady Blowing for a Low-Pressure Turbine Cascade". *Journal of Turbomachinery,* ***126***(4), pp. 560–569.

[11] Ludewig, T., Mack, M., Niehuis, R., and Franke, M., 2011. Optimization of the Blowing Ratio for a Low Pressure Turbine Cascade with Active Flow Control. ETC2011 Paper No. 131.

[12] Bons, J. P., Sondergaard, R., and Rivir, R. B., 2001. "Turbine Separation Control Using Pulsed Vortex Generator Jets". *Journal of Turbomachinery,* ***123***(2), pp. 198–206.

[13] Lengani, D., Simoni, D., Ubaldi, M., Zunino, P., and Bertini, F., 2009. "An Experimental Study of the Reynolds Number Influence on a Laminar Separation Bubble". *ERCOFTAC Bulletin,* ***80***, pp. 24–29.

[14] Ries, T., Mohr, F., Baumann, J., Rose, M., Rist, U., Raab, I., and Staudacher, S., 2009. "LP Turbine Laminar Separation With Actuated Transition: DNS, Experiment and Fluidic Oscillator CFD". In ASME Paper GT2009-59600.

[15] Gier, J., Franke, M., Hübner, N., and Schröder, T., 2008. "Designing LP Turbines for Optimized Airfoil Lift". In ASME Paper GT2008-51101.

[16] Wazzan, A. R., Okamura, T. T., and Smith, A. M. O., 1998. "SPATIAL AND TEMPORAL STABILITY CHARTS FOR THE FALKNER–SKAN BOUNDARY-LAYER PROFILES,". In *Defense Technical Information Center OAI-PMH Repository*. Defense Technical Information Center OAI-PMH Repository.

[17] Kügeler, E., Nürnberger, D., Weber, A., and Engel, K., 2008. "Influence of Blade Fillets on the Performance of a 15 Stage Gas Turbine Compressor". In ASME Paper GT2008-50748.

[18] Stadtmüller, P., Fottner, L., and Fiala, A., 2000. "Experimental and Numerical Investigation of Wake-Induced Transistion on a Highly Loadad Turbine at Low Reynolds Numbers". In ASME Paper GT2000-0269.

[19] Wright, P., 1980. "The Coanda meter – a fluidic digital gas flowmeter". *J. Phys. E: Sci. Instrum.,* ***13/4***, pp. 433–436. Vol.13.

[20] Yang, J.-T., Chen, C.-K., Tsai, K.-J., Lin, W.-Z., and Sheen, H.-J., 2007. "A novel fluidic oscillator incorporating step-shaped attachment walls". *Sensors and Actuators A: Physical,* ***135***(2), pp. 476 – 483.

[21] Khelfaoui, R., Colin, S., Orieux, S., Caen, R., and Baldas, L., 2009. "Numerical and Experimental Analysis of Monostable Mini- and Micro-Oscillators". *Heat Transfer Engineering,* ***30***(1), pp. 121–129.

[22] Chen, C.-K., Wang, L., Yang, J.-T., and Chen, L.-T., 2006. "Experimental and Computational Analysis of Periodic Flow Structure in Oscillator Gas Flow Meters". *Journal of Mechanics,* ***22***, pp. 137–144.

[23] Sim̃oes, E. W., Furlan, R., Leminski, R. E. B., Gongora-Rubio, M. R., Pereira, M. T., Morimoto, N. I., and Aviles, J. J. S., 2005. "Microfluidic Oscillator for Gas Flow Control and Measurement". *Flow Measurement and Instrumentation,* ***16***(1), pp. 7 – 12.

[24] Gebhard, U., Hein, H., and Schmidt, U., 1996. "Numerical Investigation of Fluidic Micro-Oscillators". *Journal of Micromechanics and Microengineering,* ***6***, pp. 115–117.

[25] Schreck, E., and Schäfer, M., 2000. "Numerical study of bifurcation in three-dimensional sudden channel expansions". *Computers & Fluids,* ***29***, pp. 583–593.